Activation of DNA strand exchange by cationic comb-type copolymers: effect of cationic moieties of the copolymers

Sung Won Choi[1], Arihiro Kano[1] and Atsushi Maruyama[1,2,*]

[1]Institute for Materials Chemistry and Engineering, Kyushu University, 744-CE11 Motooka, Nishi, Fukuoka 819-0395 and [2]CREST, Japan Science and Technology Agency, 4-1-8 Honcho, Kawaguchi, Saitama 332-0012, Japan

ABSTRACT

We have previously reported that poly(L-lysine)-*graft*-dextran cationic comb-type copolymers accelerate strand exchange reaction between duplex DNA and its complementary single strand by >4 orders of magnitude, while stabilizing duplex. However, the stabilization of the duplex is considered principally unfavourable for the accelerating activity since the strand exchange reaction requires, at least, partial melting of the initial duplex. Here we report the effects of different cationic moieties of cationic comb-type copolymers on the accelerating activity. The copolymer having guanidino groups exhibited markedly higher accelerating effect on strand exchange reactions than that having primary amino groups. The high accelerating effect of the former is considered to be due to its lower stabilizing effect on duplex DNA, resulting from its increased affinity to single-stranded DNA. The difference in affinity was clearly demonstrated by a fluorescence correlation spectroscopy study; the interaction of the former with single-stranded DNA still remained high even at 1 M NaCl, while that of the latter completely disappeared. These results suggest that some modes of interactions, such as hydrogen bonding, other than electrostatic interactions between the copolymers having guanidino groups and DNAs may be involved in strand exchange activation.

INTRODUCTION

An essential genetic principle is association, dissociation and strand exchange of nucleic acid hybrids. Since free nucleic acids are highly flexible macromolecules, the possibility of finding several different regions complementary to a given extent of single polynucleotide chains is quite high and will increase as the chain length increases. Therefore, proper hybridization of polynucleotide chains can easily be impeded by kinetic traps (i.e. local energy minima), which are stable enough to halt the hybridization process for a physiologically significant amount of time. These folding problems (1) such as partially hybridized or mishybridized intermediates can be overcome by the aid of specific nucleic acid chaperone proteins that prevent aggregation and dissociate the intermediate to offer the chance for another hybridization attempt (2,3). This idea was suggested for RNA by Karpel *et al.* (4) over 30 years ago. Nucleic acid chaperones are ubiquitous and abundant proteins found in all living organisms and viruses (5). The proteins interact with nucleic acids with a little or no sequence specificity. Nucleic acid chaperone activities of several proteins, including the nucleocapsid (NC) protein of human immunodeficiency virus type 1 (HIV-1) (6,7), heterogeneous nuclear ribonucleoproteins (hnRNPs) (8), and *Escherichia coli* cold shock proteins (Csps) (9), have been explored *in vitro*. These highly diverse families of nucleic acid–binding proteins possess activities enabling rapid and faithful annealing of complementary strands (10), strand transfer from one hybrid to a more-stable hybrid (11), and strand exchange between double-stranded DNA (ds DNA) and its complementary single-stranded DNA (ss DNA) (12). The activities are likely achieved by destabilizing nucleic acid hybrids, thus reducing the free energy needed for dissociation and reassociation of base pairings (1,13). Therefore, nucleic acid chaperones catalyze the folding of nucleic acids into the thermodynamically stable formations (1). Once the most stable nucleic acid structure has been reached by the proteins, their binding is no longer required to maintain the new structure (1,5).

We have previously reported that cationic comb-type copolymers (PLL-*g*-Dex) composed of a cationic poly (L-lysine) backbone (<20 wt%) and abundant hydrophilic dextran side chains (>80 wt%) form completely soluble

complexes with DNA (14–16), and stabilize DNA hybrids such as duplexes and triplexes (16,17). Our spectroscopic study indicated that the copolymers interact with DNAs without changing DNA base-pair structures (bp) (18). Recently we have shown that the copolymers produced nucleic acid chaperone-like activity; the copolymers accelerate the DNA strand exchange reaction with high sequence specificity (19–21). Interestingly, unlike naturally occurring nucleic acid chaperones, the copolymers accelerate the strand exchange reaction while stabilizing ds DNA (16,20). Thus the mechanisms involved in the chaperone-like activity of the copolymers seem markedly different from those of nucleic acid chaperone proteins. Since the strand exchange reaction requires, at least, partial melting of the initial ds DNA, the stabilization of ds DNA is considered principally unfavourable for the nucleic acid chaperone activity of the copolymer. Therefore, we expected that lowering the stabilizing effect of the cationic comb-type copolymers on ds DNA would be a strategy to increase their chaperoning activity. Considering an equilibrium state between ds DNA and ss DNA, the copolymer is required to interact preferentially with ss DNA with high affinity to reduce its duplex stabilizing effect. It is, however, general that cationic copolymers have higher affinity to ds DNA than ss DNA since the former possesses higher charge density, thereby interacting stronger through electrostatic interaction than the latter. Thus, preferential interaction with ss DNA is hard to be acquired by cationic copolymers on the basis of electrostatic interaction.

Lysine has a primary amino group as a basic functional moiety, whereas arginine has a guanidino group. Both the primary amino and the guanidino groups bear positive charges at physiological pH. It was reported that, while lysine- or arginine-rich peptides interact with DNAs predominantly through electrostatic interactions at physiological pH, stronger hydrogen bonding is involved in the interactions between arginine-rich peptides and DNAs or RNAs (22,23). In fact, it has been shown that arginine can form hydrogen bonds with bases and/or phosphates within ds DNA as well as ss DNA (24). Some reports suggested that oligolysines stabilize ds DNA against thermal denaturation more effectively than oligoarginines, although aggregation or precipitation of the resulting complex made further studies difficult (25,26). We have modified the copolymers with different cationic moieties to regulate ss DNA/ds DNA-binding selectivity. In a previous paper, we reported the preparation of cationic comb-type copolymer (GPLL-*g*-Dex) (27), having guanidino groups as a cationic moiety. The guanidination method was employed to convert the primary amino groups of lysine moieties into guanidino groups without changing the frame structures, e.g. grafting degree, chain length of backbone and side chains, of the cationic comb-type copolymers. In the present study, we studied DNA–copolymer interactions in the thoroughly soluble system by spectroscopic and calorimetric measurements, as well as DNA strand exchange reactions. The fluorescence correlation spectroscopy (FCS) using a single-molecule fluorescence detection system enabled us to directly assess the effect of the cationic moieties on the affinity of the copolymers to ss and ds DNAs. We showed that GPLL-*g*-Dex interacted with ss DNA stronger than PLL-*g*-Dex. The higher affinity of GPLL-*g*-Dex to ss DNA likely led to a decrease in its stabilizing effect on ds DNA compared to PLL-*g*-Dex, producing a markedly higher accelerating effect on strand exchange reactions than PLL-*g*-Dex.

MATERIALS AND METHODS

Materials

Poly(L-lysine) (PLL) hydrobromides of number-averaged molecular weight (M_n) = 6.5 and 27.6 kDa as salt free were purchased from Bachem Bioscience Inc. (King of Prussia, PA, USA) and Nacalai Tesque, Inc. (Kyoto, Japan), respectively. Dextran (Dex, M_n = 8.7 kDa) was obtained from Amersham Bioscience (Uppsala, Sweden). The guanidination reagent, 1-guanyl-3,5-dimethylpyrazole nitrate (GDMP), was purchased from Sigma-Aldrich (St. Louis, MO, USA). NewPol PE64 surfactant, poly-oxyethylene (M_n = 1.2 kDa) and polyoxypropylene (M_n = 1.8 kDa) block copolymer were purchased from Sanyo Chemical Industry (Kyoto, Japan). All oligonucleotides were supplied by FASMAC (Kanagawa, Japan) and their purity was analysed with a reverse phase high performance liquid chromatography on a Capcell Pak column from Shiseido (Tokyo, Japan). The primary sequences and codes of the oligonucleotides are given in Figure 1A. Concentrations of the oligonucleotide stock solutions were determined by UV absorbance and molar extinction coefficients (F1 and NF1, $1.98 \times 10^5 \, M^{-1} \, cm^{-1}$; T1 and NT1, $1.98 \times 10^5 \, M^{-1} \, cm^{-1}$; ScrF1NT1 and ScrT1NF1, $3.99 \times 10^5 \, M^{-1} \, cm^{-1}$; F2 and NF2, $2.11 \times 10^5 \, M^{-1} \, cm^{-1}$; T2 and NT2, $1.65 \times 10^5 \, M^{-1} \, cm^{-1}$; ScrF2NT2 and ScrT2NF2, $3.72 \times 10^5 \, M^{-1} \, cm^{-1}$) at 260 nm. Fluorescein 5(6)-isothiocyanate (FITC)-labeled 20-bp duplexes were obtained by mixing either F1 or F2 with each complementary strand, NT1 or NT2, in equimolar amounts and annealing at 95°C for 5 min, followed by slow cooling to room temperature over 16 h. Salmon sperm DNA of average 300-bp (c.a. 70% ds DNA) was obtained from Nichiro (Tokyo, Japan) and was used for isothermal titration calorimetry measurements. Other solvents and chemicals of reagent grade were purchased from Wako Pure Chemical Industries (Osaka, Japan) and were used without further purification.

Guanidination of the PLL-*g*-Dex comb-type copolymers

Guanidination of the copolymers was previously described in detail (27). Briefly, PLL-*g*-Dex copolymers (K7-88 and K28-83) were prepared by a reductive amination reaction of PLL (M_n = 6.5 kDa or 27.6 kDa) with Dex in sodium borate buffer (14,16). The number average molecular weight (as salt free) of the resulting K7-88 and K28-83 copolymers were 26 kDa (grafting ratio$_{Dex}$ = 10.9 mol%, dextran content = 87.7 wt%) and 95 kDa (grafting ratio$_{Dex}$ = 7.4 mol%, dextran content = 82.9 wt%), respectively. GPLL-*g*-Dex copolymers (GK7-88 or GK28-83) were obtained by the guanidination of each PLL-*g*-Dex with GDMP at 37°C and pH 9.5

for 96 h. The structural formulas of PLL-*g*-Dex and GPLL-*g*-Dex are shown in Figure 1B. The guanidination reactions were monitored with ^{1}H NMR. It was able to vary the guanidination ratios (% Gu) of the copolymers up to 100% (% Gu = 100) by controlling reaction time and reagent concentrations, where the value of % Gu was calculated with the equation shown in Figure 1B. K28-83 and GK28-83 were used in all experiments on this study except for ITC measurements.

UV-melting temperature measurements

Twenty-bp ds DNAs (NF1/NT1 and NF2/NT2) for UV-melting temperature (T_m) measurements were prepared by the method mentioned in 'Materials'. The final concentration of the ds DNA solution was adjusted to 0.69 µM (13.98 µM in bp) with 10 mM sodium phosphate buffer (pH 7.2), containing 150 mM NaCl and 0.5 mM EDTA (Buffer I). The concentrations of copolymer solutions corresponding to given N/P ratios ([Lys]$_{copolymer}$/[phosphate]$_{DNA}$ charge ratios), were adjusted with Buffer I. The solutions of ds DNA and copolymer were mixed with a micro pipette, where the N/P ratios ranged from 0 to 10. UV-melting curves of ds DNAs were recorded with a Shimadzu UV-1600 PC spectrometer (Kyoto, Japan) equipped with a TMSPC-8 temperature controller. The samples were gradually heated from 25 to 100°C at a constant rate of 1°C/min. The differential absorbance ($\Delta A = A_{260} - A_{340}$) was calculated to correct baseline shift. The first derivative [d(ΔA)/dT] was calculated from the melting-curve data. Peak temperatures in the derivative curves were designated as melting temperatures.

DNA–copolymer binding assay by fluorescence correlation spectroscopy

DNA–copolymer binding assay was carried out by fluorescence correlation spectroscopy (FCS) (28,29) with an Olympus MF20 single-molecule fluorescence detection system (Tokyo, Japan). A 24 × 16-well microplate (purchased from Olympus) was used. All samples were prepared in 10 mM sodium phosphate buffer (pH 7.2, 0.5 mM EDTA) plus 5 µg/ml NewPol PE64 surfactant (to prevent the absorption of DNA and copolymers to the surface of tubes and microplates), containing various NaCl concentrations ranging from 150 mM to 1 M. For determination of binding properties, the concentration of 5′ tetramethylrhodamine (TAMRA)-labeled 40-mer ss DNA (ScrT1NF1: scramble sequence of T1 and NF1) was kept constant at 5 nM and the concentrations of PLL-*g*-Dex or GPLL-*g*-Dex were varied in the range of 0–39 µM in their cationic group. After the mixtures were incubated for 30 min at room temperature, an aliquot (50 µl) of each sample was transferred to a microplate. A standard solution of 1 nM RITC in the same buffer was used to derive optical parameters necessary to a proper measurement. A He–Ne laser (λ_{exc} = 543 nm) was polarized in the vertical plane through the bottom of the sample plate, where laser power was set at 200 µW. All measurements were carried out in more than duplicate and five scans each lasting 10 s at room temperature

A


```
F1:     5'-TCATA ATCAG CCATA CCACA-3'-FITC
NF1:    5'-TCATA ATCAG CCATA CCACA-3'
T1:     TAMRA-5'-TGTGG TATGG CTGAT TATGA-3'
NT1:          5'-TGTGG TATGG CTGAT TATGA-3'
ScrF1NT1: 5'-TTCAG TTAGA TGTCA GATGC
             CGCTA TAGTA CCATA TCAGA-3'-FITC
ScrT1NF1: TAMRA-5'-TTCAG TTAGA TGTCA
             GATGC CGCTA TAGTA CCATA TCAGA-3'

F2:     5'-ATGGT GAGCA AGGGC GAGGA-3'-FITC
NF2:    5'-ATGGT GAGCA AGGGC GAGGA-3'
T2:     TAMRA-5'-TCCTC GCCCT TGCTC ACCAT-3'
NT2:          5'-TCCTC GCCCT TGCTC ACCAT-3'
ScrF2NT2: 5'-CTGCT CTGAG ACTAT GACTG
             ACACT GGGCC TGCGA CCGAG-3'-FITC
ScrT2NF2: TAMRA-5'-CTGCT CTGAG ACTAT
             GACTG ACACT GGGCC TGCGA CCGAG-3'
```

B

PLL-*g*-Dex

GPLL-*g*-Dex

Guanidination ratio (% Gu) = (y / (x+y)) × 100
= 28, 54, 74, or 100
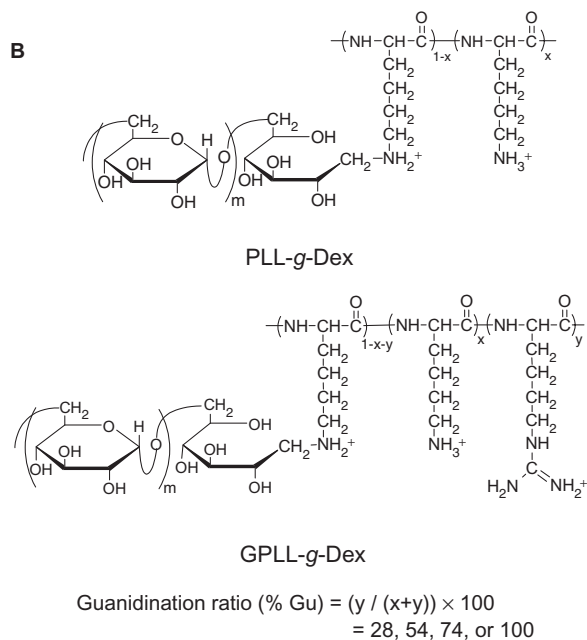
Figure 1. (**A**) Base sequences of oligonucleotides used in this study; F1 and 2: FITC-labeled sequences, NF1 and 2: non-labeled F1 and 2 sequences, T1 and 2: TAMRA-labeled sequences, NT1 and 2: non-labeled T1 and 2 sequences, ScrF1NT1, ScrT1NF1, ScrF2NT2, and ScrT2NF2: FITC or TAMRA-labeled scramble sequences of corresponding ODNs. (**B**) Structural formulas of PLL-*g*-Dex and GPLL-*g*-Dex comb-type copolymers. The level of the guanidination ratio is expressed by '% Gu' that stands for % fraction of lysine residues substituted by guanidino groups.

(25 ± 2°C). The obtained data were fitted according to an autocorrelation function embodied in the accompanying software. Each data point was mean value of all measured samples. The measurements of TAMRA-labeled 20-mer ss DNA (T1) and ds DNA (T1/NF1) were also conducted under the same conditions.

Gel shift assay for competitive binding study of ss and ds DNAs to the copolymer

FITC-labeled 20-bp ds DNA (0.56 µM, 5 pmol F1/NT1 or F2/NT2) was mixed with 40-mer ss DNA (0.56 µM,

5 pmol ScrF1NT1 or ScrF2NT2) in Buffer I. The 40-mer ss DNAs have the scramble sequences of the corresponding 20-bp ds DNAs. The mixtures were incubated either with PLL-*g*-Dex or with GPLL-*g*-Dex at N/P ratios ranging from 0 to 2 at 25°C for 1 h. After incubation, each sample was analysed by electrophoresis on 13% polyacrylamide gel at 5°C for a given time period in 89 mM Tris-borate buffer containing 2.5 mM EDTA (Buffer II). The gel was then photographed with Fujifilm LAS-3000 luminescent image analyser (Tokyo, Japan). The images were analysed by using Image Gauge Ver. 4.0 (Fujifilm, Tokyo, Japan).

Calorimetric analysis of DNA–copolymer interaction

Isothermal titration calorimetry (ITC) was performed using a VP-ITC microcalorimeter from MicroCal Inc. (Northampton, MA, USA). For the ITC measurements, PLL-*g*-Dex (K7-88) and GPLL-*g*-Dex (GK7-88) were used as ligands. DNA solution (300-bp salmon sperm DNA, c.a. 70% ds DNA) was prepared in Buffer I. Single-stranded DNA was prepared by denaturing the DNA solution at 95°C for 10 min and then quenching at room temperature. The ss DNA solution was kept at 4°C before the measurement. All solutions were degassed before titration using a ThermoVac system (MicroCal) at 20°C. DNA solutions (0.38 mM in nucleotide) were maintained in the thermostated cell (1.4 ml) at 25°C. A 250 μl syringe was used for the titrant. Mixing was effected by the syringe at 300 r.p.m. during equilibrium and experiment. Typically 20 injections of 5 μl each (13.26 mM in cationic group of PLL-*g*-Dex or GPLL-*g*-Dex in Buffer I) were performed at 4 min interval between injections in a single titration at 25°C. Dilution heats of the ligand were measured by injecting each copolymer solution into Buffer I alone and were subtracted from the binding heats. Non-linear least-squares analysis of the titration data were processed using the Origin® software (Ver. 6.0) provided with the instrument.

DNA strand exchange reaction estimated by gel electrophoresis

DNA strand exchange reactions were carried out according to previous reports (19,30). FITC-labeled ds DNA (0.56 μM, 5 pmol F2/NT2) was incubated with its non-labeled complementary ss DNA (2.8 μM, 25 pmol NF2) in Buffer I at 25°C in the absence or presence of the copolymer (N/P ratio = 2) for various time periods. After incubation, the reaction was stopped by cooling samples in an ice bath, followed by adding poly(sodium vinylsulfonate) (final 0.2 wt%) to the reaction mixtures to dissociate the copolymer from DNA (31). The mixtures were finally separated by gel electrophoresis at 100 V on a 13% polyacrylamide gel at 5°C for a given time period in Buffer II. The gel was then visualized with a Fujifilm LAS-3000 luminescent image analyser (Tokyo, Japan). The images were analysed by using Image Gauge Ver. 4.0 (Fujifilm, Tokyo, Japan). The exchange degree in percent was calculated by using the following equation to take

into account the theoretical fraction of the exchanged product under equilibrium as 100%:

$$\text{Degree of exchange}\,(\%) = (f \times ([F - ds]_0 + [ss]_0)/[ss]_0) \times 100 \qquad \mathbf{1}$$

where f is fraction of exchanged ds DNA, which is determined from the band intensity normalized using the FITC-labeled ds DNA. $[F-ds]_0$, and $[ss]_0$ are the initial concentrations of FITC-labeled duplex and its complementary ss DNA, respectively. Strand exchange reactions between F1/NT1 ds DNA and NF1 ss DNA were also conducted under the same method at 15°C.

Real-time monitoring of DNA strand exchange reaction by fluorescence resonance energy transfer assay

The real-time detection of DNA strand exchange reaction was carried out by fluorescence resonance energy transfer (FRET) assay according to previous reports (20,32). FRET-labeled ds DNA (F1/T1) solution was introduced into a quartz cuvette in the fluorescence spectrometer. A stirred solution of F1/T1 mixed with each copolymer (N/P ratio = 2) was allowed to equilibrate to the measured temperature, 15°C. Final concentration of the ds DNA was 12 nM (27 pmol), dissolved in Buffer I containing 5 μg/ml NewPol PE64 surfactant. The solution was excited at 490 nm and fluorescence emission at 520 nm was monitored with a JASCO FP-6500 spectrofluorometer (Tokyo, Japan) equipped with a temperature-controlled cell holder. Baseline emission values were first recorded for ∼10 min, and then the ss DNA solution (135 pmol M1, final concentration: 60 nM) was injected with a syringe to initiate strand exchange reaction. The value of % exchange degree was calculated with following equation:

$$\%\text{Exchange degree} = ([FI]_t - [FI]_0)/([FI]_\infty - [FI]_0) \times 100 \qquad \mathbf{2}$$

where $[FI]_0$ is the initial fluorescence intensity, $[FI]_t$ and $[FI]_\infty$ are fluorescence intensity at time t and after the reaction reached equilibrium, respectively. The value of $[FI]_\infty$ was practically obtained by heating the mixture at 90°C for 5 min followed by slow cooling to reaction temperature.

RESULTS

Effect of the guanidination on the stabilization of ds DNA

We have prepared a series of GPLL-*g*-Dex copolymers with different levels of guanidination ratios. The level of the guanidination ratio is expressed by '% Gu' which stands for % fraction of lysine residues substituted by guanidino groups (Figure 1B). The stabilizing effect of the cationic comb-type copolymers on DNA duplexes was examined by recording thermal melting profiles with a UV spectrometer. Figure 2 represents the UV-melting curves of 20-bp duplexes (NF1/NT1 and NF2/NT2) in the absence or presence of each copolymer at N/P ratio = 5. The observed helix-coil transitions were reversible, i.e. ds DNAs regenerated in the cooling scan, yielding a similar
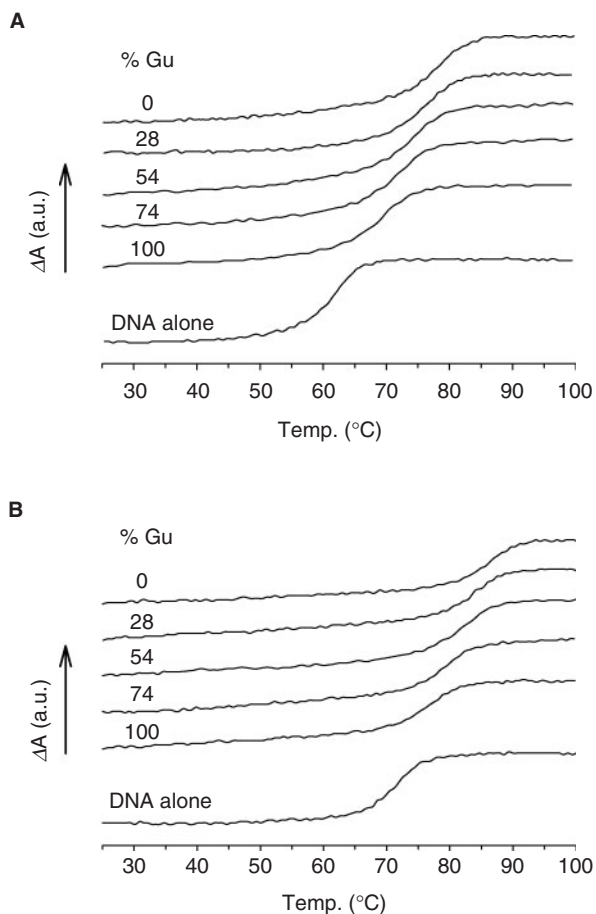
Figure 2. UV-melting temperature profiles of 20-bp ds DNA in the absence or presence of a series of guanidinated copolymers at an N/P ratio of five. The UV-melting curves of NF1/NT1 (**A**) or NF2/NT2 (**B**) were recorded from 25 to 100°C at 1°C/min in Buffer I (see 'Materials and Methods'). The concentration of ds DNA was $0.69\,\mu$M.

UV-T_m profile even in the presence of the copolymers (data not shown). An increase in the T_m values of the duplexes was observed in the presence of the copolymers, but the increment of T_m was gradually reduced with increasing guanidination ratio. Figure 3A shows T_m values of NF1/NT1 in the absence or presence of the copolymers. Free DNA underwent helix-coil transition at around 62°C. In the presence of the copolymers, the T_m values increased and then reached a plateau at N/P ratio > 2 regardless of % Gu. The results suggest that DNAs were thoroughly associated with the copolymers at N/P ratio > 2. While PLL-g-Dex, without guanidino modification, increased T_m by 16°C, GPLL-g-Dex with increasing % Gu value showed less ability to increase T_m. Especially in the case of % Gu = 100, T_m increased by only 8°C. A similar result was also obtained with a different ds DNA sequence (NF2/NT2) as shown in Figure 3B. To evaluate the contribution of guanidino groups to T_m, the T_m values at N/P ratio = 5 were plotted as a function of % Gu in Figure 3C. The T_m values of both NF1/NT1 and NF2/NT2 ds DNAs linearly decreased with an increase in % Gu from 0–100%. The results clearly show that the substitution of primary amino groups with guanidino groups on the
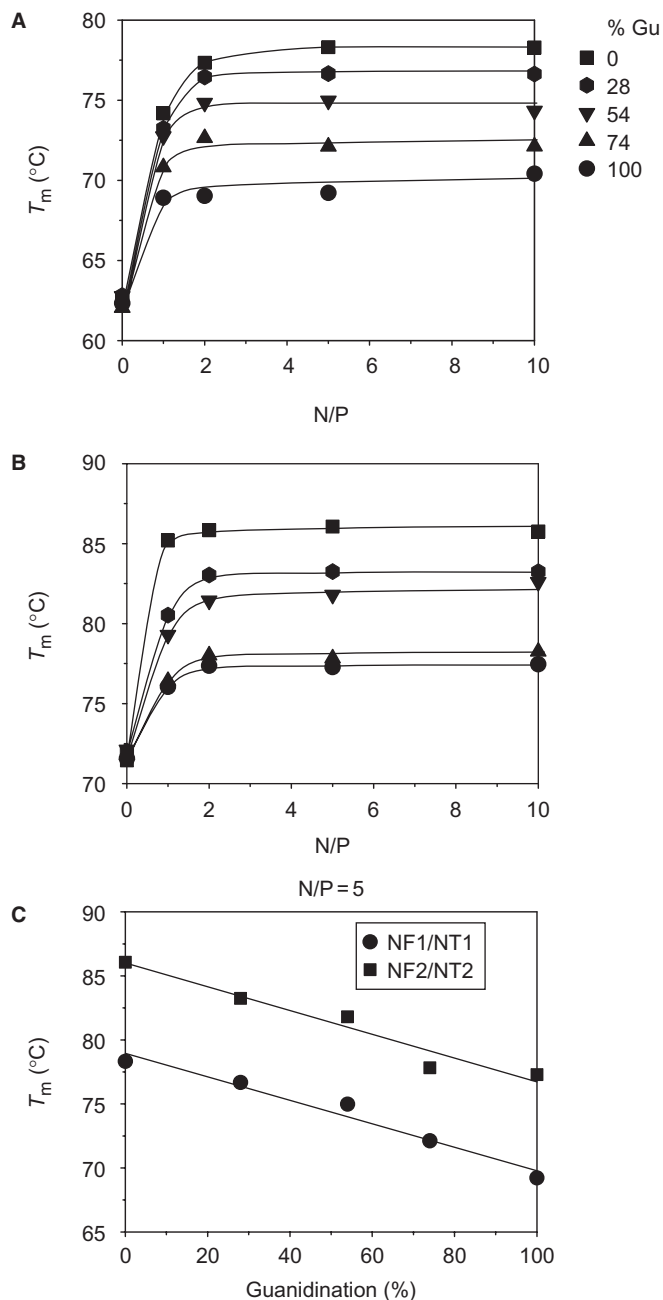

Figure 3. UV-T_m values of ds DNA in the absence or presence of a series of guanidinated copolymers. The UV-melting curves of ds DNAs were recorded at N/P ratios ranging from 0 to 10. The differential absorbance ($\Delta A = A_{260} - A_{340}$) was calculated to correct baseline shift. The first derivative [d(ΔA)/dT] was calculated from the melting-curve data. Peak temperatures in the derivative curves were designated as melting temperatures. Changes in T_m values of 20-bp ds DNAs are plotted as a function of the N/P ratios [(NF1/NT1) (**A**) or (NF2/NT2) (**B**)] and the guanidination ratio at an N/P ratio of five (**C**).

cationic comb-type copolymer backbone leads to a decrease in the stabilizing effect.

### Binding assay of the copolymer to ds DNA and ss DNA

To understand the decrease in the stabilization effect observed with the guanidination, binding assays between
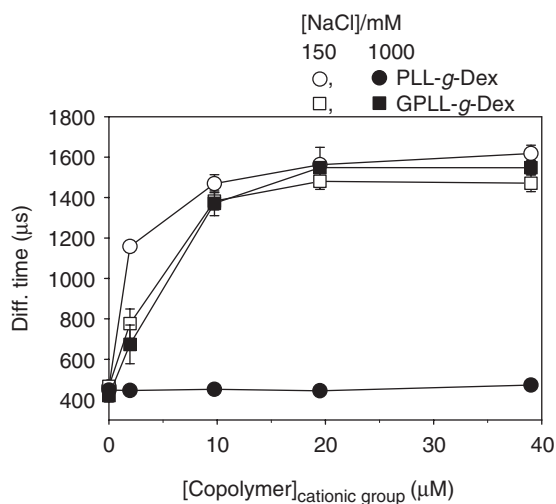
Figure 4. DNA-binding with copolymer measured by FCS. Five nM TAMRA-labeled 40-mer ss DNA (ScrT1NF1) was incubated with increasing concentrations of PLL-*g*-Dex and GPLL-*g*-Dex in 10 mM sodium phosphate buffer (see 'Materials and Methods') containing 150 mM and 1 M NaCl and measured at room temperature (25 ± 2°C).

the cationic comb-type copolymers and either ss or ds DNA were carried out by FCS (28,29). Since a diffusion time calculated by the autocorrelation analysis of the fluorescence fluctuation is proportional to the mass, the complex formation of fluorescence-labeled DNA with the copolymer leads to an increase in the diffusion time. Figure 4 illustrates the typical FCS results for the copolymer binding with TAMRA-labeled 40-mer ss DNA (5 nM, ScrT1NF1) at 150 mM and 1 M NaCl. The diffusion times of the 40-mer ss DNA alone were ca. 450 μs under these salt concentrations. At [NaCl] = 150 mM, the diffusion times increased with increasing copolymer concentration and then reached a plateau at [copolymer] > 20 μM (in cationic group), implying complete complex formation. When either 0.06 wt% sodium dodecyl sulfate or 0.07 wt% poly (sodium vinylsulfonate) (31) was added to the reaction mixtures to dissociate copolymer from DNA, the diffusion time in the presence of the copolymer got back to that of DNA alone (data not shown). Hence, the increase in the diffusion time is due to complex formation.

At [NaCl] = 1 M, an obvious difference between the binding profiles was observed. The ss DNA associated with GPLL-*g*-Dex, while it did not associate with PLL-*g*-Dex at all. This result indicates that GPLL-*g*-Dex has stronger interaction with 40-mer ss DNA than PLL-*g*-Dex. The higher affinity of GPLL-*g*-Dex to ss DNA is clearly shown in Figure 5, where the ionic strength dependencies on the DNA–copolymer interactions at [copolymer]$_{cationic\ group}$ = 19.5 μM (A, B) and 19.0 μM (C) are summarized. While the complex of PLL-*g*-Dex with 40-mer ss DNA dissociated at [NaCl] > 500 mM, that of GPLL-*g*-Dex retained up to [NaCl] = 1 M (Figure 5A). Such difference in copolymer affinity was also observed for 20-mer ss DNA (T1) as shown in Figure 5C. While PLL-*g*-Dex almost lost its binding to the ss DNA at
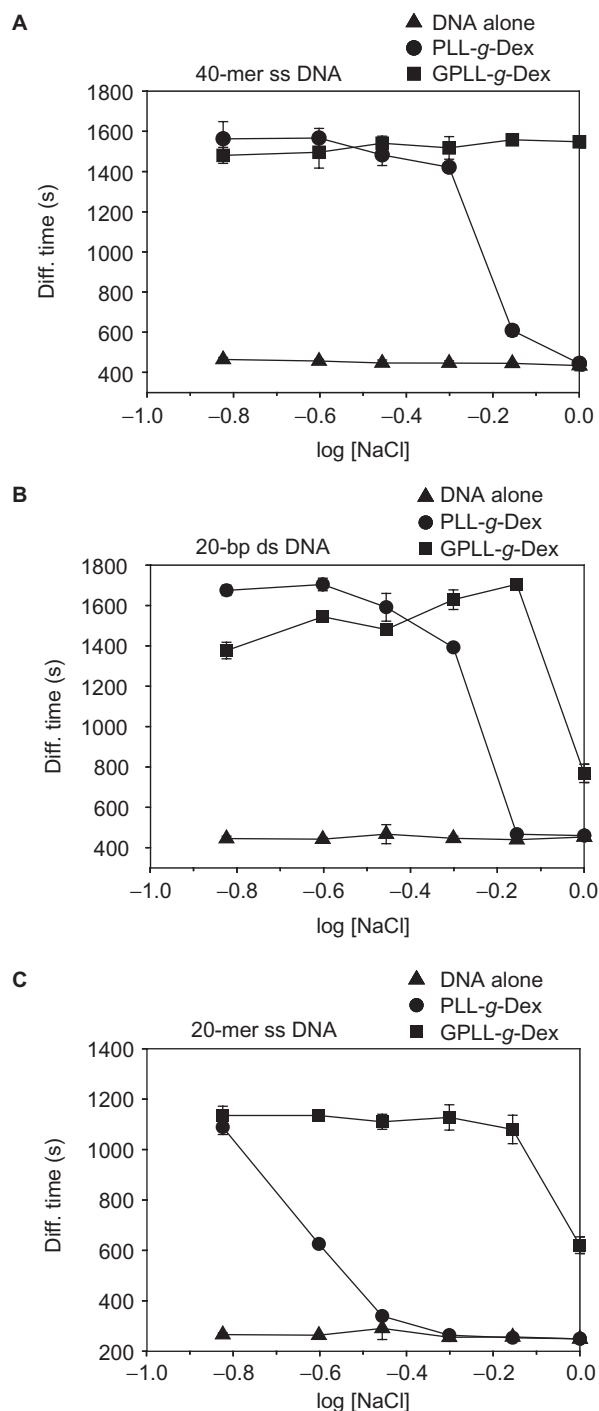
Figure 5. Ionic strength dependency of DNA–copolymer interaction. Fluorescence diffusion times of 40-mer ss DNA (ScrT1NF1) (**A**), 20-bp ds DNA (T1/NF1) (**B**) and 20-mer ss DNA (T1) (**C**) were determined by FCS in the absence or presence of PLL-*g*-Dex or GPLL-*g*-Dex under the same conditions as described in Figure 4. The copolymer concentrations were 19.5 μM (**A** and **B**) and 19.0 μM (**C**) in [copolymer]$_{cationic\ group}$.

[NaCl] > 350 mM, GPLL-*g*-Dex maintained its binding up to 700 mM NaCl. On the other hand, a minor increase in binding affinity to ds DNA (T1/NF1) by guanidination was observed (Figure 5B). Note that GPLL-*g*-Dex binding to 20-mer ss DNA is similar to that to 20-bp ds DNA
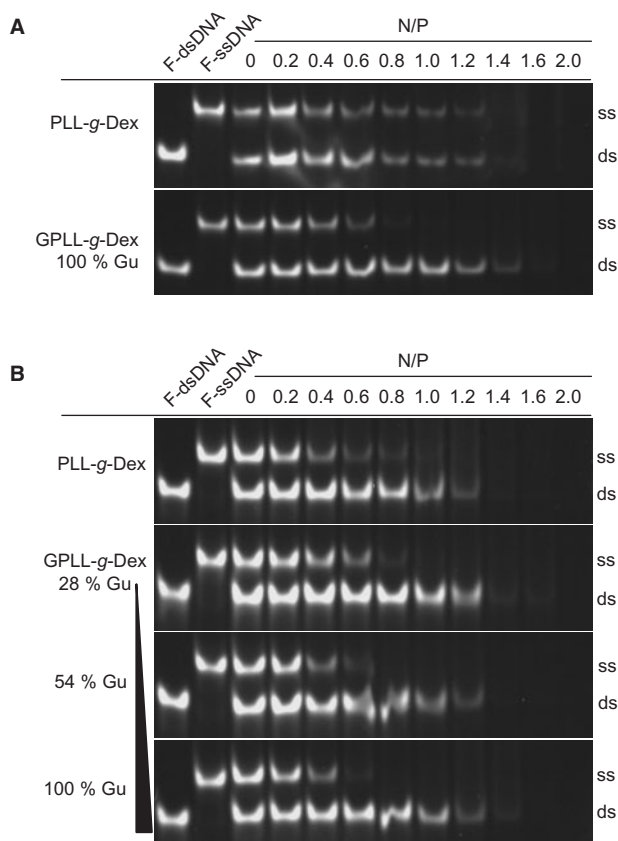
Figure 6. Competitive complex formations of copolymers with 20-bp ds DNA and 40-mer ss DNA determined by gel electrophoresis. The mixtures of 0.56 μM ds DNA (F1/NT1) (**A**) or (F2/NT2) (**B**) and 0.56 μM ss DNA (ScrF1NT1) (**A**) or (ScrF2NT2) (**B**) were incubated at 25°C in Buffer I for 1 h in the absence or presence of PLL-*g*-Dex or GPLL-*g*-Dex at a given *N/P* ratio indicated above each lane. After incubation, the mixtures were analysed by electrophoresis at 100 V on 13% polyacrylamide gel at 5°C for a given time period in Buffer II (see 'Experimental Procedures') at 5°C.

(Figure 5B and C), even though the later possesses the higher number and density of anionic charges. These results indicate again that the guanidination of PLL-*g*-Dex altered the ss/ds DNA selectivity in the complex formation. However, the difference in ss/ds affinity at 150 mM NaCl could not be estimated because of the saturated interactions of the copolymers to either ss or ds DNA. To confirm the difference in ss/ds binding affinity at 150 mM NaCl, a competitive binding study of the copolymers with ss and ds DNAs was carried out. An increasing amount of the copolymer was added to a mixture of 20-bp ds DNA and 40-mer ss DNA, and unbound DNAs were separated by polyacrylamide gel electrophoresis. As shown in Figure 6, with increasing amount of copolymers, unbound ds and ss DNAs decreased. However, the ss DNA band disappeared at lower *N/P* ratio when the guanidinated copolymer was added to the DNA mixture. The result supports the preferential binding of the guanidinated copolymers to ss DNA in 150 mM NaCl. The difference in ss/ds affinity likely explains the weaker stabilization effects of GPLL-*g*-Dex on ds DNA. Although GPLL-*g*-Dex, similar to PLL-*g*-Dex, stabilized ds DNA by reducing the counterion

condensation effect, the stronger affinity of GPLL-*g*-Dex to ss DNA over ds DNA resulted in the weaker stabilization effect (see 'Discussion').

Calorimetric study on interpolyelectrolyte complex formation

Although the DNA–copolymer binding assay suggested that GPLL-*g*-Dex has a higher affinity for ss DNA than PLL-*g*-Dex, the mechanism that underlies this behavior was unclear. To gain further insights into the behavior, DNA–copolymer complex formation was studied by ITC. ITC directly measures heat generated or absorbed upon binding. In the experiments, a copolymer solution was titrated into ss DNA or ds DNA solution. Only a small enthalpy changes ($\Delta H_{obs} < -0.4\,kcal/mol$) was detected for copolymer binding to both ss and ds DNAs, suggesting that PLL-*g*-Dex and GPLL-*g*-Dex form complex with DNA through entropy-driven manner.

Strand exchange accelerating activity of the copolymer

Since GPLL-*g*-Dex exhibited weaker stabilization effects on ds DNA than PLL-*g*-Dex, the former was expected to produce higher accelerating activity toward DNA strand exchange reactions. Figure 7A shows the time course of strand exchange reactions between FITC-labeled ds DNA (F2/NT2) and its complementary ss DNA (NF2) in the absence or presence of either PLL-*g*-Dex or GPLL-*g*-Dex (% Gu = 100) at 25°C. The slower and faster migration bands correspond to unreacted F2/NT2 ds DNA and F2 ss DNA dissociated from the ds DNA, respectively. The exchange degree shown in Figure 7C was determined using Equation (1) as described in 'Materials and Methods'. The DNA strand exchange reaction in the absence of the copolymers was hardly detected even after 24 h incubation. On the other hand, the reaction was accelerated by both PLL-*g*-Dex and GPLL-*g*-Dex. Especially, the drastic effect of GPLL-*g*-Dex was observed. While it took 3 h for PLL-*g*-Dex to reach a 50% strand exchange degree, only 5 min was enough for GPLL-*g*-Dex to obtain a similar exchange level (Figure 7A and C). Apparent rates of the exchange reaction were determined by pseudo-first-order kinetic analyses (Figure 7C). It was revealed that the strand exchange reaction rate accelerated by GPLL-*g*-Dex is > 30 times higher than that by PLL-*g*-Dex.

The accelerating effect of the copolymers on the reaction between F1/NT1 ds DNA and NF1 ss DNA was also observed under the same experimental conditions at 25°C. We found that the reactions were much faster compared to those observed between F2/NT2 and NF2 (data not shown). Even if the reaction was carried out at 15°C, as shown in Figure 7B and D, the exchange degrees in the presence of either PLL-*g*-Dex or GPLL-*g*-Dex rapidly reached > 60% level within 5 min incubation and a difference in the accelerating effect between the copolymers could not be determined under the conditions. The difference in strand exchange rates between F1/NT1/NF1 and F2/NT2/NF2 reaction systems probably results from difference in ds DNA stability. F1/NT1 duplex that has a lower melting temperature (lower GC content) than F2/NT2 duplex would be more reactive for strand exchange.
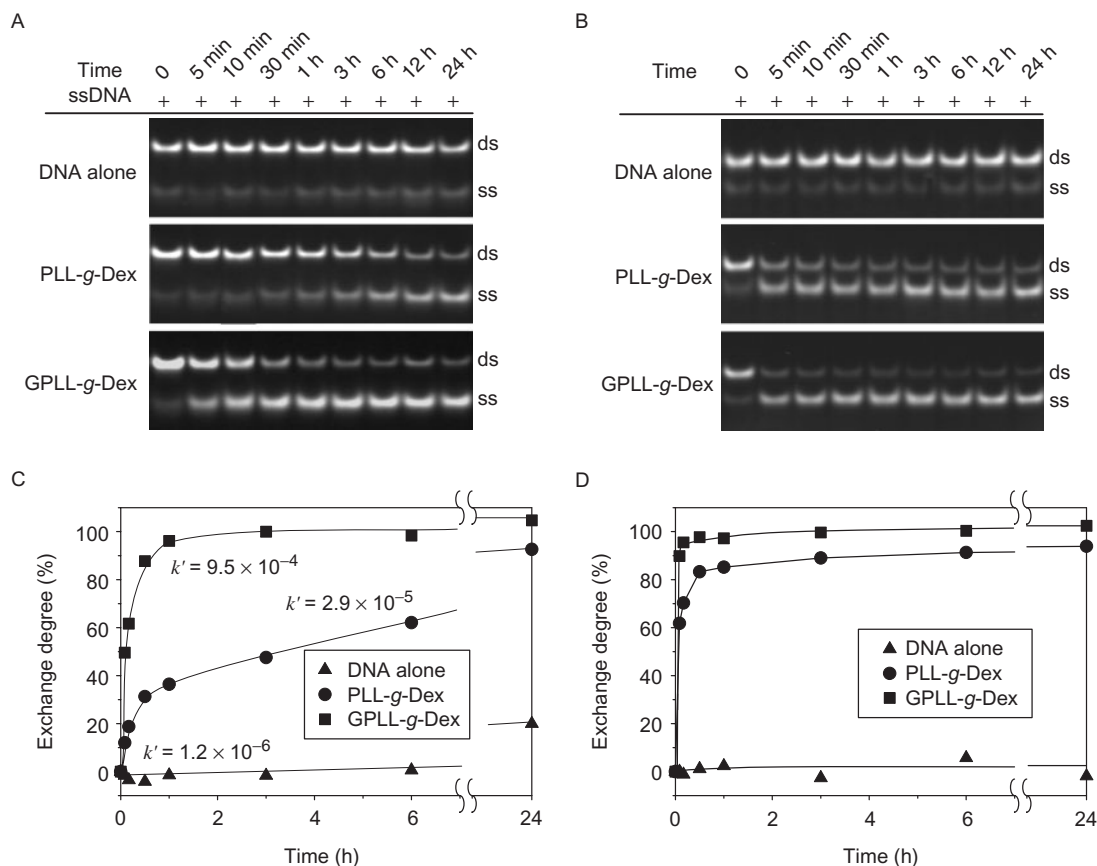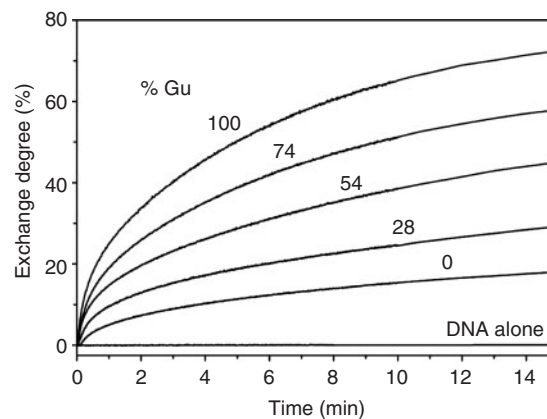
Figure 7. Strand exchange reaction between ds DNA and ss DNA in the absence or presence of PLL-*g*-Dex or GPLL-*g*-Dex. (**A**) FITC-labeled ds DNA (0.56 μM F2/NT2) was incubated at 25°C with ss DNA (2.8 μM NF2) in Buffer I in the absence or presence of the copolymers (*N/P* ratio = 2) for various time periods indicated above each lane. After the incubation, 0.2 wt% poly(sodium vinylsulfonate) was added to dissociate each copolymer from DNA before electrophoresis. Gel electrophoresis was carried out at 100 V on a 13% polyacrylamide gel at 5°C for a given time period in Buffer II (see 'Materials and Methods'). (**B**) Strand exchange reaction between FITC-labeled ds DNA (F1/NT1) and ss DNA (NF1) at 15°C. Other conditions are the same as (**A**). The values of % exchange degree of F2/NT2 with NF2 (**C**) and F1/NT1 with NF1 (**D**) are plotted as a function of reaction time, where the % exchange degree were calculated by Equation (1). Values of k' (s^{-1}) represent the pseudo-first-order rate constants for the strand exchange between F1/T1 and NT1 (**C**).

Since the gel electrophoresis method has limitations for evaluating kinetics in such a rapid exchange reaction shown in Figure 7B and D, we adopted FRET method (20,32) at a 50 times lower DNA concentration than that used for the gel electrophoresis. Figure 8 shows the time courses of the reaction of F1/T1 with NT1 at 15°C in the absence or presence of the cationic comb-type copolymers, monitored by FRET assay. The exchange degree was determined using Equation (2) as described in 'Materials and Methods'. The reaction was further accelerated with increasing the level of guanidination (% Gu). While PLL-*g*-Dex (%Gu = 0) accelerates the exchange reaction by three orders, GPLL-*g*-Dex (%Gu = 100) does it by more than four orders (Table 1). The observation clearly demonstrates that the substituted guanidino groups contribute to increasing the accelerating effect of cationic comb-type copolymer.

DISCUSSION

We previously reported that the comb-type copolymers having guanidino groups were prepared by simple reaction

Figure 8. Time course of strand exchange reaction between ds DNA and ss DNA in the absence or presence of PLL-*g*-Dex or GPLL-*g*-Dex monitored by FRET assay. A stirred solution of ds DNA (F1/T1) was mixed with each copolymer (*N/P* ratio = 2) at 15°C. Final concentration of ds DNA was 12 nM (27 pmol) in Buffer I. The solution was excited at 490 nm and fluorescence emission was monitored at 520 nm. The strand exchange reaction was started by adding ss DNA solution (135 pmol NT1, final concentration: 60 nM) with a syringe. The value of % exchange degree was calculated by Equation (2).

method, where the primary amino groups of lysine moieties (PLL-*g*-Dex) were converted into guanidino groups (GPLL-*g*-Dex) (27). This method allows us to estimate the effect of the cationic moieties without changing other primary structures of the copolymer, such as grafting degree or the lengths of main and graft chains. In the present study, we showed that the stabilizing effect of PLL-*g*-Dex decreased with an increase in the guanidination degree (Figures 2 and 3).

The high electrostatic potential from polyelectrolytes results in the accumulation of counterions in the immediate vicinity of the polyelectrolytes. As anionic charge density of nucleic acids increases upon DNA hybridization such as duplex and triplex formation, an increasing fraction of counterions is attracted. Delocalization (condensation) of counterions in the vicinity of DNA strands is entropically unfavourable under low or physiological salt condition, so that the DNA hybridization is hindered by the counterion condensation effect (33,34). The interaction of oppositely charged substances to the DNA causes a perturbation of the electrostatic potential surrounding the polyelectrolyte. This perturbation leads to release of the condensed counterions. Thus, the complex formation between negatively charged DNA and positively charged polyelectrolyte is thermodynamically driven by entropic contribution from release of the condensed counterions. Simultaneously, the release of the counterion condensed on DNA leads to the stabilization of duplex and triplex DNAs (35). Since a guanidino group is a stronger base than a primary amino group, the ability of GPLL-*g*-Dex to reduce the counterion condensation effect is the same or higher, compared to that of PLL-*g*-Dex. Hence, the weaker stabilization activities of GPLL-*g*-Dex can not be explained on the basis of the counterion condensation effect. The FCS measurements clearly showed that the affinity of GPLL-*g*-Dex for ss DNA is significantly higher than that of PLL-*g*-Dex (Figures 4 and 5). The higher affinity for ss DNA of GPLL-*g*-Dex than of PLL-*g*-Dex shifts the helix-coil DNA equilibrium toward the ss DNA coil state, explaining the weaker stabilizing effect of the former than the latter (Figures 2 and 3). The mechanisms involved in different affinity between PLL-*g*-Dex and GPLL-*g*-Dex has remained still unclear. However, it is likely that hydrogen-bonding interaction produced by guanidino groups plays a role (22–24). Single-stranded DNA could provide more sites for hydrogen-bonding interaction than ds DNA. Furthermore, flexibility of ss DNA is favourable for the copolymer to form hydrogen bonding that requires particular geometric arrangements of hydrogen-donor and acceptor groups (36).

The results of ITC measurements showed no significant difference in the enthalpy change accompanying complex formation between PLL-*g*-Dex with either ss or ds DNA (data not shown). This observation is consistent with the previous reports on the electrostatic binding of polycationic substances to DNA (37–39), which is characteristic for interpolyelectrolyte complex formation driven through entropic contribution. Although additional interactions involving hydrogen bonding (22–24,36) and other interactions are expected to contribute to the complex

Table 1. Strand exchange rate constant in the absence or presence of the copolymers

% Gu	Strand exchange rate constant, k' [s^{-1}][a]	$k'(+)/k'(-)$[a]
DNA alone	1.9×10^{-7}	1
0	5.7×10^{-4}	3.1×10^3
28	9.8×10^{-4}	5.3×10^3
54	1.7×10^{-3}	9.3×10^3
74	2.9×10^{-3}	1.5×10^4
100	4.4×10^{-3}	2.4×10^4

[a]Values of k' represent the pseudo-first-order rate constants for the strand exchange between F1/T1 ds DNA and NT1 ss DNA in the absence [$k'(-)$] and presence [$k'(+)$] of either PLL-*g*-Dex or GPLL-*g*-Dex at $N/P = 2$, respectively. Regression parameters, r^2, in pseudo-first-order analyses were over 0.95 for all rate constant determination.

formation between GPLL-*g*-Dex and DNA, their thermodynamic effect could not be detected.

The strand exchange reaction under our experimental conditions is initiated by the spontaneous and partial unwinding (breathing) of the initial duplex to form a branched nucleation complex with the complementary strand, followed by branch migration (21,30). In the reaction, the nucleation process is reported to be the rate-determining step (30). PLL-*g*-Dex likely facilitates the strand exchange reaction by promoting the branched nucleation complex formation (16, 20). In the present study, we showed that the strand exchange reaction was further facilitated by GPLL-*g*-Dex. The strand exchange reaction rate increased proportionally to the increment of the guanidination ratio, in accordance with a decrease in the stabilization effect on ds DNA. Taking these observations into account, it is considered that the rate-determining process is shifted to the initial breathing step in the presence of the cationic copolymer.

The present study demonstrated that the cationic moieties of the comb-type copolymers influence the ss/ds DNA selectivity of the copolymers, ds DNA stabilizing and strand exchange reaction accelerating effects. It is unique that a structural difference in cationic moieties on the copolymer backbone still produces the remarkable effects regardless of the abundant graft chains that could impede close association of the cationic backbone with DNAs. Further study on the cationic comb-type copolymers with different primary structure will allow us to design artificial materials capable of manipulating hybridization of nucleic acid.

ACKNOWLEDGEMENTS

REFERENCES

1. Herschlag,D. (1995) RNA chaperones and the RNA folding problem. *J. Biol. Chem.*, **270**, 20871–20874.
2. Todd,M.J., Lorimer,G.H. and Thirumalai,D. (1996) Chaperonin-facilitated protein folding: optimization of rate and yield by an iterative annealing mechanism. *Proc. Natl Acad. Sci. USA*, **93**, 4030–4035.
3. Csermely,P. (1999) Chaperone-percolator model: a possible molecular mechanism of Anfinsen-cage-type chaperones. *BioEssays*, **21**, 959–965.
4. Karpel,R.L., Swistel,D.G., Miller,N.S., Geroch,M.E., Lu,C. and Fresco,J.R. (1975) Acceleration of RNA renaturation by nucleic acid unwinding proteins. *Brookhaven Symp. Biol.*, **26**, 165–174.
5. Cristofari,G. and Darlix,J.-L. (2002) The ubiquitous nature of RNA chaperone proteins. *Prog. Nucleic Acid Res. Mol. Biol.*, **72**, 223–268.
6. Tsuchihashi,Z., Khosla,M. and Herschlag,D. (1993) Protein enhancement of hammerhead ribozyme catalysis. *Science*, **262**, 99–102.
7. Herschlag,D., Khosla,M., Tsuchihashi,Z. and Karpel,R.L. (1994) An RNA chaperone activity of non-specific RNA binding proteins in hammerhead ribozyme catalysis. *EMBO J.*, **13**, 2913–2924.
8. Bertrand,E.L. and Rossi,J.J. (1994) Facilitation of hammerhead ribozyme catalysis by the nucleocapsid protein of HIV-1 and the heterogeneous nuclear ribonucleoprotein A1. *EMBO J.*, **13**, 2904–2912.
9. Jiang,W., Hou,Y. and Inouye,M. (1997) CspA, the major cold-shock protein of *Escherichia coli*, is an RNA chaperone. *J. Biol. Chem.*, **272**, 196–202.
10. Darlix,J-L., Lapadat-Tapolsky,M., de Rocquigny,H. and Roques,B.P. (1995) First glimpses at structure-function relationships of the nucleocapsid protein of retroviruses. *J. Mol. Biol.*, **254**, 523–537.
11. Lapadat-Tapolsky,M., Pernelle,C., Borie,C. and Darlix,J.-L. (1995) Analysis of the nucleic acid annealing activities of nucleocapsid protein from HIV-1. *Nucleic Acids Res.*, **23**, 2434–2441.
12. Urbaneja,M.A., Wu,M., Casas-Finet,J.R. and Karpel,R.L. (2002) HIV-1 nucleocapsid protein as a nucleic acid chaperone: spectroscopic study of its helix-destabilizing properties, structural binding specificity, and annealing activity. *J. Mol. Biol.*, **318**, 749–764.
13. Rein,A., Henderson,L.E. and Levin,J.G. (1998) Nucleic-acid-chaperone activity of retroviral nucleocapsid proteins: significance for viral replication. *Trends Biochem. Sci.*, **23**, 297–301.
14. Maruyama,A., Katoh,M., Ishihara,T. and Akaike,T. (1997) Comb-type polycations effectively stabilize DNA triplex. *Bioconjugate Chem.*, **8**, 3–6.
15. Sato,Y., Kobayashi,Y., Kamiya,T., Watanabe,, H. Akaike,T., Yoshikawa,K. and Maruyama,A. (2005) The effect of backbone structure on polycation comb-type copolymer/DNA interactions and the molecular assembly of DNA. *Biomaterials*, **26**, 703–711.
16. Maruyama,A., Watanabe,H., Ferdous,A., Katoh,M., Ishihara,T. and Akaike,T. (1998) Characterization of interpolyelectrolyte complexes between double-stranded DNA and polylysine comb-type copolymers having hydrophilic side chains. *Bioconjugate Chem.*, **9**, 292–299.
17. Maruyama,A., Ohnishi,Y., Watanabe,H., Torigoe,H., Ferdous,A. and Akaike,T. (1999) Polycation comb-type copolymer reduces counterion condensation effect to stabilize DNA duplex and triplex formation. *Colloids Surf. B.*, **16**, 273–280.
18. Sato,Y., Moriyama, R. Choi,S.W., Kano,A. and Maruyama,A. (2007) Spectroscopic investigation of cationic comb-type copolymers/DNA interaction: interpolyelectrolyte complex enhancement synchronized with DNA hybridization. *Langmuir*, **23**, 65–69.
19. Kim,W.J., Ishihara,T., Akaike,T. and Maruyama,A. (2001) Comb-Type cationic copolymer expedites DNA strand exchange while stabilizing DNA duplex. *Chem. Eur. J.*, **7**, 176–180.
20. Kim,W.J., Akaike,T. and Maruyama,A. (2002) DNA strand exchange stimulated by spontaneous complex formation with cationic comb-type copolymer. *J. Am. Chem. Soc.*, **124**, 12676–12677.
21. Kim,W.J., Sato,Y., Akaike,T. and Maruyama,A. (2003) Cationic comb-type copolymers for DNA analysis. *Nat. Mater.*, **2**, 815–820.
22. Cotton,F.A., Day,V.W., Hazen,E.E., Jr and Larsen,S. (1973) Structure of methylguanidinium dihydrogen orthophosphate. Model compound for arginine-phosphate hydrogen bonding. *J. Am. Chem. Soc.*, **95**, 4834–4840.
23. Pörschke,D. (1978) Thermodynamic and kinetic parameters of oligonucleotide–oligopeptide interactions. Specificity of arginine·inosine association. *Eur. J. Biochem.*, **86**, 291–299.
24. Lancelot,G., Mayer,R. and Helene,C. (1979) Models of interaction between nucleic acids and proteins. hydrogen bonding of arginine with nucleic acid bases, phosphate groups and carboxylic acids. *Biochim. Biophys. Acta*, **564**, 181–190.
25. Inoue,S. and Ando,T. (1970) Interaction of clupeine with deoxyrinonucleic acid. I. Thermal melting and sedimentation studies. *Biochemistry*, **9**, 388–394.
26. Olins,D.E., Olins,A.L. and von Hippel,P.H. (1967) Model nucleoprotein complexes: studies on the interaction of cationic homopolypeptides with DNA. *J. Mol. Biol.*, **24**, 157–176.
27. Choi,S.W., Sato,Y., Akaike,T. and Maruyama,A. (2004) Preparation of cationic comb-type copolymer having guanidino moieties and its interaction with DNAs. *J. Biomat. Sci. Polym. Ed.*, **15**, 1099–1110.
28. Elson,E.L. and Madge,D. (1974) Fluorescence correlation spectroscopy. I. Conceptual basis and theory. *Biopolymers*, **13**, 1–27.
29. Hess,S.T., Huang,S., Heikal,A.A. and Webb,W.W. (2002) Biological and chemical applications of fluorescence correlation spectroscopy: a review. *Biochemistry*, **41**, 697–705.
30. Reynaldo,L.P., Vologodskii,A.V., Neri,B.P. and Lyamichev,V.I. (2000) The kinetics of oligonucleotide replacements. *J. Mol. Biol.*, **297**, 511–520.
31. Ferdous,A., Watanabe,H., Akaike,T. and Maruyama,A. (1998) Poly(L-lysine)-graft-dextran copolymer: amazing effects on triplex stabilization under physiological pH and ionic conditions (in vitro). *Nucleic Acids Res.*, **26**, 3949–3954.
32. Bazemore,L.R., Takahashi,M. and Radding,C.M. (1997) Kinetic analysis of pairing and strand exchange catalyzed by RecA. Detection by fluorescence energy transfer. *J. Biol. Chem.*, **272**, 14672–14682.
33. Record,M.T., Jr. (1975) Effects of sodium and magnesium ions on the helix-coil transition of DNA. *Biopolymers*, **14**, 2137–2158.
34. Manning,G.S. (1969) Limiting laws and counterion condensation in polyelectroyte solutions. I. Colligative properties. *J. Chem. Phys.*, **51**, 924–933.
35. Lohman,T.M., deHaseth,P.L. and Record,M.T., Jr. (1980) Pentalysine-deoxyribonucleic acid interactions: a model for the general effects of ion concentrations on the interactions of proteins with nucleic acids. *Biochemistry*, **19**, 3522–3530.
36. Cheng,A.C., Chen,W.W., Fuhrmann,C.N. and Frankel,A.D. (2003) Recognition of nucleic acid bases and base-pairs by hydrogen bonding to amino acid side-chains. *J. Mol. Biol.*, **327**, 781–796.
37. Bronich,T., Kabanov,A.V. and Marky,L.A. (2001) A thermodynamic characterization of the interaction of a cationic copolymer with DNA. *J. Phys. Chem. B.*, **105**, 6042–6050.
38. Pozharski,E. and MacDonald,R.C. (2002) Thermodynamics of cationic lipid-DNA complex formation as studied by isothermal titration calorimetry. *Biophys. J.*, **83**, 556–565.
39. Ross,P.D. and Shapiro,J.T. (1974) Heat of interaction of DNA with polylysine, spermine, and Mg^{++}. *Biopolymers*, **13**, 415–416.